

Knowledge-Spreader: Learning Facial Action Unit Dynamics with Extremely Limited Labels

Xiaotian Li, Xiang Zhang, Taoyue Wang, Lijun Yin

State University of New York at Binghamton

Abstract. Recent studies on the automatic detection of facial action unit (AU) have extensively relied on large-sized annotations. However, manually AU labeling is difficult, time-consuming, and costly. Most existing semi-supervised works ignore the informative cues from the temporal domain, and are highly dependent on densely annotated videos, making the learning process less efficient. To alleviate these problems, we propose a deep semi-supervised framework **Knowledge-Spreader (KS)**, which differs from conventional methods in two aspects. First, rather than only encoding human knowledge as constraints, KS also learns the Spatial-Temporal AU correlation knowledge in order to strengthen its out-of-distribution generalization ability. Second, we approach KS by applying consistency regularization and pseudo-labeling in multiple student networks alternately and dynamically. It spreads the spatial knowledge from labeled frames to unlabeled data, and completes the temporal information of partially labeled video clips. Thus, the design allows KS to learn AU dynamics from video clips with only **one label** allocated, which significantly reduce the requirements of using annotations. Extensive experiments demonstrate that the proposed KS achieves competitive performance as compared to the state of the arts under the circumstances of using only **2%** labels on BP4D and **5%** labels on DISFA. In addition, we test it on our newly developed large-scale comprehensive emotion database, which contains considerable samples across well-synchronized and aligned sensor modalities for easing the scarcity issue of annotations and identities in human affective computing. The code and new database will be released to the research community.

Keywords: Semi-supervised learning, facial action unit detection, knowledge distillation, sparsely labeled data, Spatial-Temporal, pseudo-labeling

1 Introduction

Understanding human facial action dynamics is crucial for human-computer interaction (HCI), which reflects the individuals' affective states to enhance the affinity of communication. Facial action unit (AU) detection plays a vital role in automatic facial action analysis. Over the past few years, a substantial amount of works [11] [47] [1] based on deep learning have shown the superior power of constructing informative features against the traditional methods. The majority of the recent advances [22] [43] [27] [6] [39] [48] [12] in this area

are heavily relied on large-scale labeled datasets for achieving remarkable learning performance. However, a lab-controlled AU video typically contains thousands of frames that need to be densely labeled by human annotators. As a result, datasets for dynamic facial action detection suffer high redundancy both content-wise and annotation-wise.

There are only limited works attempting to mitigate the demand for dense AU occurrence annotations. For example, the researchers [41] [46] [32] [31] summarize the distribution from existing ground-truth AU labels as the prior for detecting AUs with partially labeled data. However, the approaches of applying the distribution prior may fall into sub-optimal due to lacking adaptation mechanism. Deep semi-supervised learning has become a new choice to overcome these issues for their powerful representation and generalization ability. The existing deep semi-supervised learning methods can be roughly categorised into three methods (i.e. generative method, consistency regularization method, and pseudo-labeling methods). Recently, some hybrid methods attract the attention from many researchers. MixMatch [23] combines entropy minimization and consistency regularization in a unified loss function. FixMatch [37] combines consistency regularization and pseudo-labeling considering both labeled and unlabeled data should be trained simultaneously. Whereas, applying these image-level models to dynamic datasets is challenging due to some nuisance factors such as motion blur, video defuse, and frequent pose occlusions. Besides, human facial action characteristics present strong dependencies and mutual exclusive relation among spatially local regions [21]. For instance, the AU1 and AU2 are usually co-existence due to the constraint of facial muscles. Some recent works [24] [3] prove that the relationship of different AUs in temporal domain is also an important factor for robust AU detection. Both of the two factors have been studied for fully supervised methods, but there lacks a framework to explore if learning both spatial and temporal AU correlation knowledge can boost the semi-supervised process.

In this paper, we propose an end-to-end trainable framework **Knowledge-Spreader** (KS) for learning semi-supervised facial action dynamics. Knowledge-Spreader improves conventional semi-supervised learning in three ways. First, different from previous video-level works that need fully supervisory information or at least a few labeled frames as input segments, KS just needs limited sparsely labeled video clips, with only one label allocated. This alleviates the demand on densely labeled data effectively. Second, incorporating the weak supervisory information from both human prior and AU correlation knowledge makes KS more efficient and robust for inferring out-of-distribution information. KS learns both spatial and temporal AU correlation knowledge by transformers. The powerful generalization capability of deep learning can reduce some side effects caused by incorrect knowledge summarized by humans. For instance, some AU intensity estimation works [50] assume that there are only one peak or valley in a video sequence, while ignore the special situation that multiple peaks and valleys exist in a video. Third, our work improves the hybrid semi-supervised method (consistency regularization and pseudo-labeling) to a video level model

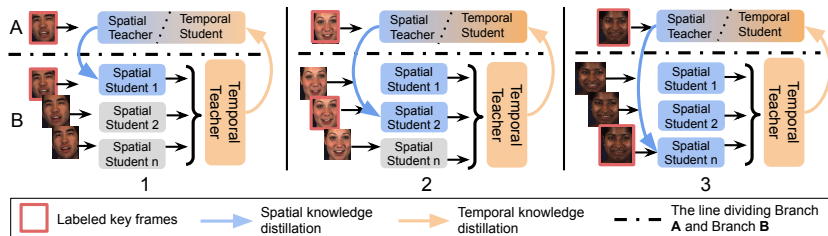


Fig. 1: Overall pipeline of Knowledge Spreading. (1) Train a Spatial Teacher for learning supervised image-level spatial knowledge in Branch *A* (*qualitative training*), and train a group of Spatial Students for semi-supervised learning in Branch *B* (*quantitative training*). (2) Process spatial knowledge distillation [10] when one of the Spatial Students gets labeled key frames (red square) as inputs while other Spatial Students infer pseudo labels using unlabeled frames. With the position of key frame shifting from 1 to 3 repeatedly, the spatial AU knowledge (blue) will be gradually spread to every Spatial Student and boost the *quantitative training* of pseudo-labeling. (3) By completing and encoding the outputs of all Spatial Students, Temporal Teacher is deployed to learn the AU temporal cues (orange). (4) Distill it back to Temporal Student in A for getting an optimal fusion of Spatial-Temporal information.

by introducing an operation “Knowledge Spreading”. The overall pipeline of Knowledge Spreading is shown in Figure 1. The *qualitative training* in Figure 1 refers that the network is trained with a small amount of labeled images, while the *quantitative training* indicates the training with a large-sized unlabeled data. Our contribution lies in three-fold: (1) We propose a deep semi-supervised architecture for AU detection by jointly utilizing the learned Spatial-Temporal AU correlation knowledge and human knowledge. (2) This is the first work to incorporate knowledge spreading by dynamic knowledge distillation and temporal confirmed pseudo-label in a self-supervised manner, to learn spatio-temporal information using extremely limited single-frame labeled video clips. (3) We have built a new spontaneous emotion database by capturing 3D geometric facial sequences, 2D facial videos, thermal videos, and physiological data sequences from 233 participants across two years period. The new database will be released to the research community along with the paper being published.

2 Related Work

2.1 Automatic Facial AU Detection

Different from general computer vision tasks, facial AUs are defined to be associated with atomic local facial muscles, which in turn correspond to the appearance features of different regions in the face. Thus, previous research [53] [42] [35] [43] [52] has extensively studied how to use manually-defined regions, local

patches, facial landmarks, heatmap, attention mechanism, and other methods to localize detailed facial parts. However, considering the structural information and dependencies among different AUs, conventional CNN is criticized to be incapable of fully characterizing their correlations. Recent advances [6] [40] [48] [12] [17] start to explore the AU relations by using data distribution, conditional random field, Bayesian Network, graph neural networks, attention mechanism, and other approaches. [3] [19] [26] attempt to integrate the inter-relationship of AUs on both spatial and temporal dimensions for learning more robust AU dependencies.

Some of the existing semi-supervised or self-supervised methods [22] [43] [27] [6] still rely on large-sized annotations and extra unlabeled data. Only a small amount of research has attempted to ease the intensive demand for AU annotations. [41] and [46] summarize the distribution from ground-truth AU labels as the prior for detecting AUs with limited labeled data with semi-supervised learning. [32] [31] leverage the joint distribution of features, AUs, and facial expression to explore the global dependencies among them. Different from all aforementioned works, KS can learn the informative Spatial-Temporal cues from sparse annotations by incorporating dynamic knowledge distillation and pseudo label.

2.2 Semi-supervised learning

Semi-supervised learning is an approach to combine a few labeled data with a large amount of unlabeled data during training. Deep semi-supervised learning is a fast-growing field with a wide broad of practical applications. FixMatch [37] has been proved to be a simple but efficient SSL method by combining both consistency regularization and pseudo-labeling. Noisy Student improves the idea of self-training and distillation with the use of noise added to the student networks. However, these works are incapable to capture the facial action dynamics as an image-level model. Recent works [36] [44] [30] propose to recognize actions from only a handful of sparsely labeled videos with the rich supervisory information in a semi-supervised way. Unlike these approaches that still need continuous and dense annotation, we aim to allocate only single-frame label for each video clip to handle the condition that the labels are extremely sparse, missing, or scarce.

3 Methodology

3.1 Overview

Our goal is to detect facial action units with video clips with single-frame labels. Specifically, we assume the facial action labels in training data are available every k frames. The i th video clip consisted of n frames is a set $V^i = \{F_{u,1}^i, F_{u,2}^i, \dots, F_{l,m}^i, \dots, F_{u,n}^i\}$ where F_u^i means unlabeled frame and F_l^i means labeled frame. Knowledge-Spreader is consisted of three key modules: (1) Spatial-Temporal information learning module (SIL), (2) knowledge spreading module

(KSM), and (3) temporal confirmed pseudo-label module (TPL). The network structure of KS is depicted in Figure 2.

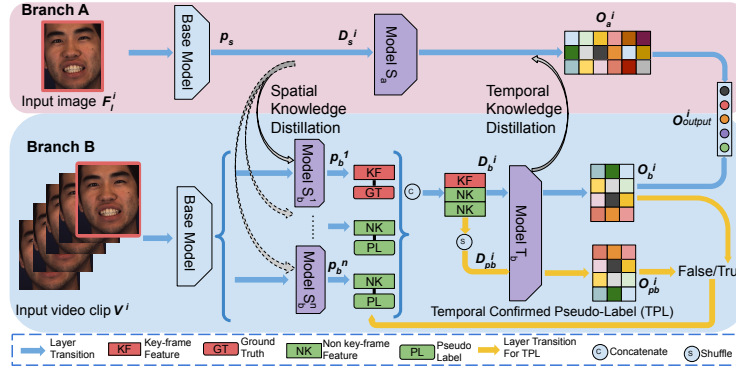


Fig. 2: **Illustration of the detailed architecture for Knowledge-Spreader.** The framework is consisted of two branches without sharing weights for learning image-level and video-level features respectively. Model S_a , S_b , and T_b (purple) are networks used for learning Spatial-Temporal AU correlation knowledge. Two level distillation (grey) and pseudo-labeling (green) consist the proposed “knowledge spreading”. A self-supervised module “temporal confirmed pseudo-label” (yellow) is designed for sensing the temporal perturbation and selecting pseudo labels with high confidence. Details are described in Section 3.1.

Spatial-Temporal Information Learning (SIL) SIL is an self-attention-based module for learning semi-supervised AU dependencies in both spatial and temporal domain. Transformers have been proved to be an effective method of learning informative temporal context in natural language processing. In order to address the limitation of applying conventional transformers on computer vision, ViT [7] splits an image into fixed-sized patches to linearly embed them with position embedding. We extend the original ViT to learn the semantic relationship of AUs in both spatial-wise and temporal-wise. As shown in Figure 2, the features from branch A and branch B are extracted by base models which are ResNet-18 [9] pre-trained on ImageNet [33]. Model S_a is designed for learning the spatial AU correlation. We firstly decouple the extracted global features p_s into multiple branches by applying global-average-pooling. The collection of decoupled features is represented as $D_s = \{f_s^1, f_s^2, \dots, f_s^u\}$ where u means the number of facial action units. Afterward, we assign u 1D learnable positional embedding to be added with these features as AU-specific embedding. Then, the AU-specific embedding sequence is fed to a standard Transformer encoder for learning the spatial-wise AU correlation knowledge. Note that, the module does

not need any extra classification token, for no obvious performance gains are observed by applying this design. Likewise, the temporal model T_b in branch B also adopts the same model design. The collection of frame-specific features is depicted as $D_b = \{p_b^1, p_b^2, \dots, p_b^n\}$ where n is the number of frames in each input sequence. The frame-specific features are extracted by the sub-networks in S_b^n and added with the corresponding temporal embedding.

Knowledge Spreading Module (KSM) KSM is the core module of the proposed Knowledge-Spreader. Inspired by FixMatch, our model also adopts a hybrid semi-supervised learning method by combining consistency regularization and pseudo-labeling. In this paper, we improve it to a video level method in the purpose of learning efficient AU dynamics. We approach KSM by several main steps: (1) train a group of Spatial Students S_b which accommodate all the frames of input sequence, (2) let the length of input clip equals to the number of Spatial Students, (3) couple the input image in branch A with the key frame of input video clip in branch B , (4) shift the location of key frame during training different batch of training samples, and (5) process distillation when Spatial Student gets the key frames, otherwise process pseudo-labeling. Furthermore, in terms of the distillation, we adopt two-level and bidirectional knowledge distillation design. The first level is from Spatial Teacher S_a to Spatial Students S_b . For the MLP-based Spatial Students S_b , we apply data random augmentation and model dropout as the noise. We assume the knowledge learned by Spatial Teacher without noise is consistent with that learned by noisy Spatial Students. The second level is from Temporal Teacher T_b to Temporal Student S_a . Instead of applying any artificial perturbation for temporal distillation, we utilize the original difference of input data for T_b and S_a . We assume the spatial knowledge learned by S_a should be consistent with the temporal knowledge learned by T_b . Thus, our model forces the Temporal Student S_a to learn the temporal AU knowledge harder, even if it only gets the image-level inputs. Here, Model S_a plays different roles in the two level distillation. Inspired by recent work [8], we adopt an online distillation method using KL divergence. The KL divergence loss in this work is used to minimize the probability distribution of student networks and their corresponding ensembles. The KL loss function of spatial knowledge distillation is defined as

$$L_{skd} = \frac{1}{b} \left(\sum_{i=1}^n T^2 KL(p_i, q_i) + \sum_{i=1}^n T^2 KL(w_i^m, q_i) \right) \quad (1)$$

where b is the batch size, T is the temperature parameter. p and w denote the soften probability distribution calculated by the Spatial Teacher S_a and one Spatial Student selected from $\{S_b^1, S_b^2, \dots, S_b^n\}$. The soft target q is expressed as $q = \text{softmax}(z_s/T)$ where z_s is performed by the mean pooling of the outputs from both S_a and one selected S_b . m is the key frame position used for controlling which Spatial Student is selected as the target of knowledge spreading. m equals $B \bmod n$, where B is the B th batch of training samples, n is the clip length. In

this paper, temperature parameter is set as 1. The KL loss function of temporal knowledge distillation is defined as

$$L_{tkd} = \frac{1}{b} \left(\sum_{i=1}^n T^2 KL(p_i, q_i) + \sum_{i=1}^n T^2 KL(w_i, q_i) \right) \quad (2)$$

p and w denote the soften probability distribution calculated by the Temporal Teacher T_b and the Temporal Student S_a respectively. Considering the data imbalance issues from skewing the training process and affect the performance of the model. We choose weighted BCE with logits as the multi-label classification loss of student networks and the function can be described as:

$$L_{bce} = -w[y \log \sigma(x) + (1 - y) \log(1 - \sigma(x))] \quad (3)$$

where x refers to the output O_a and O_b for the loss function L_s and L_t in Equation (4). x also refers to the final ensemble output O_{output} for L_{bce} in Equation (7). $\sigma(x)$ is the corresponding predicted probability. y is the AU occurrence ground truth. The loss functions of spatial knowledge distillation and temporal knowledge distillation are expressed as:

$$L_s = \sum_{i=1}^z L_{bce}^i + \alpha L_{skd}, L_t = \sum_{i=1}^z L_{bce}^i + \alpha L_{tkd} \quad (4)$$

where α is the trade-off weight, z is the number of student networks. Although branch B contains multiple student networks $\{S_b^1, S_b^2, \dots, S_b^n\}$, only one of them is selected for calculating the loss function at the same time. Thus, z equals 2. In this paper, α is set as 0.5.

Pseudo-label [15] is a simple but efficient formulation of training models in a semi-supervised way. We deploy it to train the Spatial Students in $\{S_b^1, S_b^2, \dots, S_b^n\}$ when unlabeled frames are assigned as the input. Note that, the labeled data and unlabeled data are jointly trained. The loss function is defined as

$$L_{pdbce} = -w[\hat{y} \log \sigma(x) + (1 - \hat{y}) \log(1 - \sigma(x))] \quad (5)$$

where \hat{y} denotes the pseudo labels of unlabeled frames by picking up the class which has the maximum predicted probability. The total loss function of semi-supervised learning can be denoted as

$$L_{semi} = \sum_{i=1}^{n-1} L_{pdbce}^i \quad (6)$$

Temporal Confirmed Pseudo-label (TPL) We exploit a simple self-supervised method for confirming confident pseudo labels by predicting if the features have any temporal perturbation. The smooth evolution of facial muscles leads that the facial appearance also moves gradually and smoothly over time. Thus, the

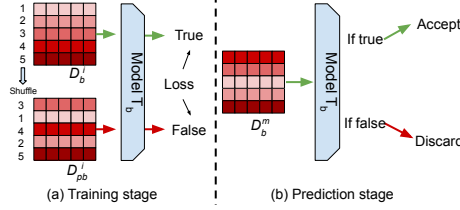


Fig. 3: Pipeline of the temporal confirmed pseudo-label. The module is based on self-supervised learning for a binary classification task. At training stage, it feeds D_b^i (without shuffling) and D_{pb}^i (shuffling D_b^i along the timeline of the features) into the model. At the prediction stage, we let the feature D_b^m (without shuffling) as the input. If it is classified as false, the corresponding pseudo labels will be discarded and vice versa. The training stage starts from the first epoch. By observation, we find the simple binary classifier takes only one or two epochs to convergence. Thus, we set the third epoch as the flag to start the prediction stage.

pseudo labels generated by incorrect features contains anomalies in the temporal domain. Researchers [44] utilize the self-supervised sequential perturbation to improve their model’s robustness and generalization. Inspired by this work, we use the temporal feature shuffling to simulate the sequential perturbation and generate negative feature samples. Although a few video clips contain fully still frames which may diminish the contribution of temporal feature shuffling, they only occupy a small portion in the whole dataset. In addition, these samples do not contain any temporal information. Therefore, labeling them incorrectly does not affect the learning ability of the spatial model. The auxiliary task is defined as a binary classification task that is jointly trained with the AU classifier on Model T_b . L_{ssl} denotes the loss of the binary classification task. Specifically, We first label the i th collection of sequential features D_b^i as true while the shuffled feature collection D_{pb}^i as false. Afterward, D_b^i and D_{pb}^i are sequentially fed into Model T_b . The loss L_{ssl} encourages the model to classify them correctly. Figure 3 illustrates the pipeline of the proposed module. As shown in Figure 6, the negative samples show the irregular pattern that AU occurs and disappears repeatedly in a short-term period. By detecting the temporal perturbation of the features and filtering out untrustable pseudo labels, TPL relieves the confirmation bias issue existing in conventional pseudo-labeling methods.

Overall loss function and algorithm The total loss is composed of the losses from previous sections, as follows:

$$L_{total} = \lambda_1 L_s + w_{ramp} (L_{bce} + \lambda_2 L_t + \lambda_3 L_{ssl} + \lambda_4 L_{semi}) \quad (7)$$

where w_{ramp} is a ramp-up function to make sure the semi-supervised learning and self-supervised learning converge relatively slowly compared with the fully-

supervised task. It is inspired by [14]. The function μ , as a simple Gaussian curve function, is defined as:

$$w_{ramp} = \exp\left(-\omega\left(1 - \frac{(x - \mu)^2}{\sigma^2}\right)\right) \quad (8)$$

where x is the epoch number. In this paper, we set $\omega = 2$, $\mu = 0$, and $\sigma = 5$. Here the w_{ramp} is set as 1 after 5 epochs' warming-up for getting the optimal effect. The algorithm of KS is shown in Algorithm 1.

Algorithm 1 Pseudocode of Knowledge-Spreader

Require: The input frame F_l^i , the input clip V^i and its frame number N , the position of key frame m . B means the B th batch of training sample. Functions of the models in branch A: base model $b_\theta(x)$, Model S_a $f_\theta(x)$. Functions of the models in branch B: base model $b_\sigma(x)$, sub-networks in S_b^i with supervision $l_\sigma(x)$ and pseudo-labeling $k_\sigma(x)$, The AU detection classifier of Model T_b $f_\sigma(x)$ and the binary classifier for self-supervised learning $g_\sigma(x)$.

```

1: for each epoch  $E$  do
2:   for each mini-batch  $b$  do
3:      $O_{abase}^i \leftarrow b_\theta(F_l^i); O_{bbase}^{(i,n)} \leftarrow b_\sigma(V^i)$ 
4:      $O_a^i \leftarrow f_\theta(O_{abase}^i)$ 
5:     for  $q = 1, \dots, N$  do
6:       if  $q == B \bmod N$  then
7:          $O_k^i \leftarrow l_\sigma(O_{bbase}^{(i,q)})$ 
8:         process spatial KD with  $O_a^i$  and  $O_k^i$ 
9:       else
10:        process pseudo-labeling with  $O_{ps}^{(i,n-1)} \leftarrow k_\sigma(O_{bbase}^{(i,q)})$ 
11:      end if
12:    end for
13:     $O_{bti}^i \leftarrow \text{Concatenate}(O_{ps}^{(i,n-1)}, O_k^i)$ 
14:     $O_b^i \leftarrow f_\sigma(O_{bti}^i)$ 
15:     $O_{pb}^i \leftarrow f_\sigma(\text{Shuffle}(O_{bti}^i))$ 
16:     $O_{ssl}^i \leftarrow g_\sigma(O_b^i = 0, O_{pb}^i = 1)$ 
17:    if  $E \leq 2$  or  $O_{ssl}^i == 1$  then
18:      Let the weight of  $L_{semi}$ ,  $\lambda_4 = 0$ 
19:    end if
20:    process temporal KD with  $O_b^i$  and  $O_a^i$ 
21:     $O_{output}^i \leftarrow \text{MeanValue}(O_b^i, O_a^i)$ 
22:    Update  $\theta$  and  $\sigma$  via SGD of Equation (7)
23:  end for
24: end for

```

4 Experiments

4.1 Datasets

BP4D and **DISFA**: BP4D [49] and DISFA [25] are widely used benchmark databases for dynamic AU detection. We followed the experimental setting of the previous work [17] to evaluate our approach for a fair comparison.

New MME: The existing facial action datasets are limited in terms of subjects number, diversity, and metadata. Thanks to the existing available multi-modal datasets [49] [51], we extend to develop a new larger-scale multi-modal

emotion (MME) database, which consists of **233** participants (132 females and 101 males). The data is significantly expanded in terms of participants number as compared to the existing databases: DISFA (27 subjects) [25], MMI (44 subjects) [29], BP4D (41 subjects) [49], BP4D+ (140 subjects) [51]. Following ethical principles, our data collection was approved by the institutional review board (IRB). Each subject signed an informed consent form. A professional performer/interviewer applied a procedure containing 10 seamlessly-integrated tasks as [49] [51] that resulted in effective elicitation of spontaneous emotions. The dataset was well-synchronized and aligned with multi-modalities including 3D geometric facial model, 2D facial videos, thermal videos, and physiology data sequences (*e.g.* heart rate, blood pressure, skin conductance (EDA), and respiration rate). Around 94,000 frames were well-annotated by three expert FACS coders for AU coding. More details are described in the supplemental material. The new database is ready for public and will be released to the research community by the time of the paper being published.

4.2 Implementation Details

We process the image by cropping off redundant area which is not relevant to face recognition. Then the images are resized to $224 \times 224 \times 3$ ($H \times W \times C$) to fit the model. Each of the training images is randomly rotated, flipped horizontally, and with color jitters (saturation, contrast, and brightness) for data augmentation. We choose SGD as the optimizer with a learning rate of 0.01 for 50 epochs. The model was implemented with Pytorch framework. The hyper-parameters in Equation (7) are set as $\lambda_1 = 0.5$, $\lambda_2 = 0.5$, $\lambda_3 = 0.2$, and $\lambda_4 = 0.25$. We use video clips with 5 frames for learning the temporal information.

4.3 Model analysis

Comparison with semi-supervised methods Figure 4 shows the performance comparison with semi-supervised methods from two areas (AU detection and general action recognition). We carefully investigated the existing works that adopt limited labels for AU detection. BGCS [46] and DAUR [41] are selected for comparison. Figure 4 (d), (e), and (f) shows the proposed model achieves significant performance improvement. Considering our foundation model may have advantages in generalization ability, we can compare the performance trend. With the available labels decreasing (from 90% to 50%), Knowledge-Spreader shows no obvious performance attenuation. Note that some other semi-supervised models from [32] [43] [27] [5] are not selected for comparison considering they use full annotation pools, extra data, or other jointly trained tasks. We further report the comparison results with some semi-supervised methods from general action recognition for a comprehensive evaluation, including Pseudo-label [15], FixMatch [37], and a video-level TCL [36]. Compared with the conventional setting of previous AU works [46] [41] [31] [32], the percentages of available AU annotations are significantly reduced (1%, 2%, 5%, 10%, 20%, 50%, 60%, 70%, 80%, 90%, and 100%) to explore where the limit of KS is. Figure 4 (a), (b), and

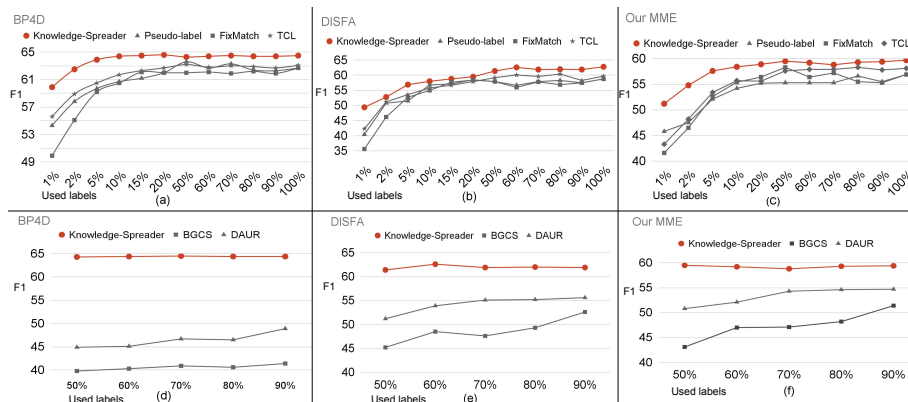


Fig. 4: Comparison with other advanced semi-supervised algorithms using different percentages of labels on BP4D, DISFA, and MME.

(c) shows prominent improvement of KS, especially when extremely limited annotations are available (1%, 2%, 5%, 10%, 15% and 20% on BP4D; 1%, 2%, and 5% on DISFA; 1%, 2%, 5%, 10%, 15% and 20% on MME). More quantitative reports are shown in the supplementary.

Table 1: Comparison with state-of-the-art methods using F1 score. The left table indicates other methods using 100% labeled data. The right table indicates a baseline model (left) and the proposed KS (right) using different percentages of labels. Underlines indicate the best result of other methods. Bold numbers indicate KS surpasses others’ best results. B and D indicates BP4D and DISFA.

Model	Reference	BP4D	DISFA	Model	B	D	Model	B	D
JAA [35]	ECCV’18	60.0	56.0	EAC (1%) [20]	43.8	31.8	KS (1%)	59.9	49.4
DSIN [4]	ECCV’18	58.9	53.6	EAC (2%)	48.7	33.3	KS (2%)	62.5	52.8
LP [28]	CVPR’19	61.0	56.9	EAC (5%)	52.2	39.4	KS (5%)	63.9	56.9
ARL [34]	AC’19	61.1	58.7	EAC (10%)	54.8	43.9	KS (10%)	64.4	58
SRERL [18]	AAAI’19	62.1	55.9	EAC (15%)	55.0	45.1	KS (15%)	64.5	58.8
UGN [38]	AAAI’21	63.3	60.0	EAC (50%)	55.6	48.0	KS (50%)	64.3	61.4
SEV [48]	CVPR’21	63.9	58.8	EAC (60%)	55.9	48.7	KS (60%)	64.4	62.6
HMP-PS [40]	CVPR’21	63.4	61.0	EAC (100%)	<u>56.3</u>	<u>51.2</u>	KS (100%)	64.5	62.8
FAUDT [12]	CVPR’21	<u>64.2</u>	<u>61.5</u>						

Comparison with supervised methods We report the results under two training setups as [45]: (1) Compare KS against the fully-supervised state-of-the-art methods with 100% labeled data. (2) Compare KS against a supervised counterpart under different training label ratios. As shown in Table 4, a collection of recent and strong benchmark algorithms are selected for better evaluation.

Table 2: Comparison with state-of-the-art methods using F1 score in terms of individual AUs. The upper part is the F1 score on BP4D; The bottom part is the F1 score on DISFA. Bold numbers indicate the best performance.

Model	Used labels	AU1	AU2	AU4	AU6	AU7	AU10	AU12	AU14	AU15	AU17	AU23	AU24	Avg.
ARL	100%	45.8	39.8	55.1	75.7	77.2	82.3	86.6	58.8	47.6	62.1	47.4	55.4	55.4
SRERL	100%	46.9	45.3	55.6	77.1	78.4	83.5	87.6	63.9	52.2	63.9	47.1	53.3	62.9
UGN	100%	54.2	46.4	56.8	76.2	76.7	82.4	86.1	64.7	51.2	63.1	48.5	53.6	63.3
HMP-PS	100%	53.1	46.1	56.0	76.5	76.9	82.1	86.4	64.8	51.5	63.0	49.9	54.5	63.4
FAUDT	100%	51.7	49.3	61.0	77.8	79.5	82.9	86.3	67.6	51.9	63.0	43.7	56.3	64.2
Our KS	15%	58.7	50.3	62.0	79.5	75.4	84.9	87.1	65.9	45.5	62.9	48.3	53.3	64.5
Our KS	100%	55.1	48.9	56.2	77.3	81.8	83.3	86.4	62.6	51.9	61.3	51.0	58.3	64.5

Model	Used labels	AU1	AU2	AU4	AU6	AU9	AU12	AU25	AU26	Avg.
ARL	100%	43.9	42.1	63.6	41.8	40.0	76.2	95.2	66.8	58.7
SRERL	100%	45.7	47.8	59.6	47.1	45.6	73.5	84.3	43.6	55.9
UGN	100%	43.3	48.1	63.4	49.5	48.2	72.9	90.8	59.0	60.0
HMP-PS	100%	38.0	45.9	65.2	50.9	50.8	76.0	93.3	67.6	61.0
FAUDT	100%	46.1	48.6	72.8	56.7	50.0	72.1	90.8	55.4	61.5
Our KS	15%	41.7	53.5	69.7	41.3	46.2	72.0	92.3	54.0	58.8
Our KS	100%	53.8	59.9	69.2	54.2	50.8	75.8	92.2	46.8	62.8

Knowledge-Spreader outperforms all other advances using only 10% labels on BP4D and 60% labels on DISFA. KS still performs competitively using only 2% labels on BP4D and 5% labels on DISFA. In addition, the experiment conducted with 100% labels shows the effectiveness of Knowledge-Spreader in a supervised manner, where the main contribution comes from Spatial-Temporal information learning module. Especially, it shows that KS surpasses the best benchmark (FAUDT) by 1.3 f1-score on DISFA. Table 5 further shows the comparison results in terms of individual AUs. The proposed method performs best on 8 out of 12 AUs on BP4D and 3 out of 8 AUs on DISFA.

4.4 Data Structure Analysis

Through the statistical experiments, we find the non-overlapping AU annotations (different AU combinations) account for only a small proportion of the overall frames number (1693 out of 140,000 frames in BP4D, 102 out of 130,000 frames in DISFA, 748 out of 94,000 frames in MME). A large number of similar labels and data densely exist across adjacent frames. It reveals that why using only a few **sparsely sampled** clips and annotations can achieve competitive or even better performance, which is consistent with the “less is better” principle from [16]. Different from existing video-level semi-supervised works [2] [44] [36] [13] that adopt continuous annotations, we sparsely sample the annotations and allocate only one annotation for every k frames. Figure 5 demonstrates that applying our method can reserve more non-overlapping AU annotations than conventional approaches with using the same number of annotations. Consequently, by utilizing abundant non-overlapping AU annotations, semi-supervised models testing on BP4D and MME is relatively more robust to resist the interference caused by missing annotations.

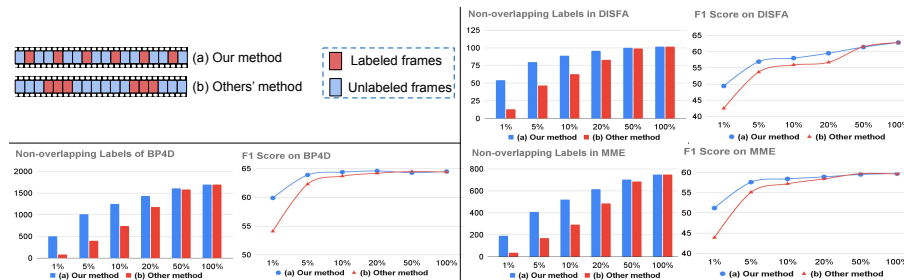


Fig. 5: Evaluation of the label sampling methods. The left top (a) indicates our strategy, and (b) indicates the conventional method. The left bottom, right top, and right bottom show the quantitative statistics of non-overlapping labels and the performance comparison of KS using different methods on BP4D, DISFA, and MME. X-axis refers to the percentage of used labels.

4.5 Ablation study

Table 3: Ablation study on BP4D, DISFA, and MME using F1 score. Bold numbers indicate the best performance.

Modules	BP4D (5%)	DISFA (5%)	MME (5%)	BP4D (50%)	DISFA (50%)	MME (50%)
Knowledge-Spreader	63.9	56.9	57.6	64.3	61.4	59.5
KSM+TPL	61.6	54.8	55.5	62.8	60.2	58.1
SIL+TPL	61.7	54.6	55.8	62.5	60.1	57.7
SIL+KSM	62.6	55.1	55.2	63.7	60.6	58.4

Effect of the Spatial-Temporal information learning module (SIL): We replace the Transformer-based SIL design with a vanilla MPL module to learn the spatial information and integrate them for learning temporal cues for a fair comparison. As shown in Table 3, the simple design leads to obvious performance degradation of KS due to being incapable of learning the AUs correlation knowledge.

Effect of the knowledge spreading module (KSM): We keep the design of key frame shifting operation, while remove the spatial knowledge and temporal knowledge distillation by setting the corresponding loss L_s and L_t to be unavailable. As a core module of Knowledge-Spreader, it plays an important role in fully spreading the AU semantic knowledge. There is an obvious performance gap between the model with and without KSM. For instance, without this module, the F1 score decreases 2.2, 2.3, and 1.8 on three databases with 5% labeled data. Similarly, it decreases 1.8, 1.3, and 1.8 with 50% labels. It demon-



Fig. 6: Pseudo labels discarded by TPL. The dotted and solid circles indicate the occurrence of AU6 and AU23. “GT” and “PL” indicate the ground-truth and the pseudo labels. Red number means incorrect pseudo labels. The ground-truth labels usually present constant pattern with no change (GT of AU6 in this figure) or simple changes (GT of AU 23 in this figure), while the incorrect pseudo labels (PL of AU6 and AU23) with temporal perturbation show the pattern that AU occurs and disappears repeatedly in a short-term period.

states that the performance degradation of the model without KSM becomes more serious as the affordable labels decrease.

Effect of the temporal confirmed pseudo-label (TPL): As shown in Table 3, with the assistant of TPL, the performance of KS is improved under different circumstances. In addition, we compare the accuracy of pseudo labels generated by TPL and naïve pseudo-label design on BP4D using 10% labels. We get 76.35% accuracy with TPL and 73.36% with the original pseudo-label, which shows the TPL achieves prominent improvement by discarding the incorrect pseudo labels with temporal perturbation. A sample is given in Figure 6 to illustrate how TPL senses and processes the incorrect pseudo labels. All the above ablation studies prove that our complete model performs the best by integrating the three key components.

5 Conclusion

In this paper, we propose a new unified Knowledge-Spreader architecture to learn the interactive Spatial-Temporal correlation knowledge with sparsely labeled videos by incorporating dynamic knowledge distillation, pseudo-labeling, and AU semantic encoding modules. Results show that the proposed model using extremely limited annotations achieves superior performance than existing methods. Comprehensive studies have demonstrated the key factor that leads to the success of Knowledge-Spreader in terms of model design and data structure, in hope of inspiring future works. In addition, a large-scale dataset for spontaneous and dynamic facial action analysis is introduced to alleviate the scarcity issue of AU annotation and subject samples. In the future, we plan to explore the application of Knowledge-Spreader on multi-modal recognition tasks. This material is based on the work supported by the US National Science Foundation.

6 Supplementary of Model Design

6.1 Details of the Spatial-Temporal Information Learning Module

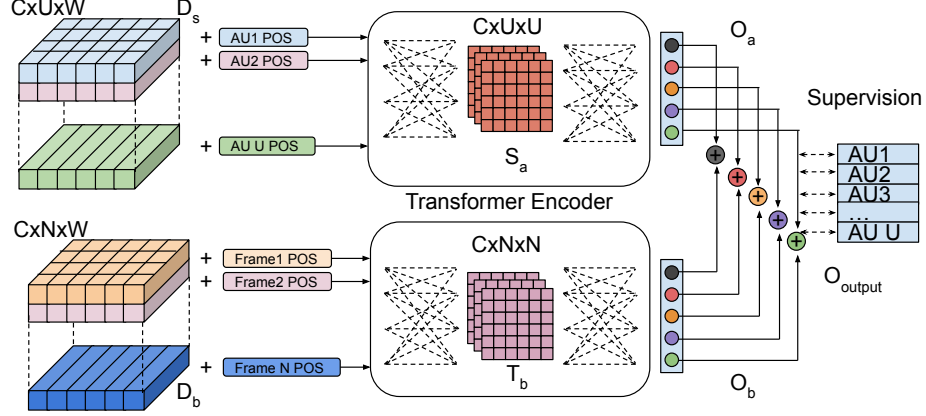


Fig. 7: Illustration of transformer-based model S_a and model T_b for learning spatial and temporal AU correlation.

The Spatial Teacher (or Temporal Student) S_a and the Temporal Teacher T_b , in Figure 7, are designed for modeling the relationships between AUs in both the intra-frame and inter-frame levels. In Spatial-Temporal Information Learning (SIL) module, we first assign U 1D learnable AU positional embedding to be added with input feature set D_s as AU-specific embedding, where U means the number of facial action units. For u th AU-specific features, a ViT transformer encoder S_a generate a set of query, key, and value tensors (Q_u, K_u, V_u), each with dimension $\mathbb{R}^{C \times W}$. Afterwards, a $C \times U \times U$ learnable attention matrix is obtained as follows:

$$A^u = \text{softmax} \left(\frac{Q_u K_u^U}{\sqrt{H}} \right) \quad (9)$$

Similarly, we assign N 1D learnable frame positional embedding to be added with input feature set D_b as frame-specific embedding, where N means the length of the input sequence. For n th frame in a sequence, another set of query, key, and value tensors (Q_n, K_n, V_n) are generated with the dimension $\mathbb{R}^{C \times W}$. A $C \times N \times N$ attention matrix is obtained as follows:

$$A^n = \text{softmax} \left(\frac{Q_n K_n^N}{\sqrt{H}} \right) \quad (10)$$

Through a series of dimensional changes, model S_a and T_b outputs U dimensional tensors O_a and O_b respectively. Finally, we take the mean ensemble output O_{output} of O_a and O_b for multi-label prediction.

Besides, we design N small-sized MLP-based models for the Spatial Students S_b . The dimension of each output feature p_b for Spatial Student is $C \times 1 \times W$.

6.2 Q&A for Model Design and Experiments

In this section, we explain some doubts of the model design and experiments.

Why the knowledge spreading operation matters for semi-supervised learning? How to maximize the use of a small but credible learned knowledge to spread into a large amount of unknown data is the core problem solved by KS. The dynamic knowledge spread with two-level distillation, which can also be seen as a two-level lever, can allow KS to transform a few spatial knowledge into a large amount of spatial knowledge, and then form more temporal knowledge. Compared with static knowledge distillation, dynamic knowledge spread contains multiple level of leverage to infer more out-of-distribution knowledge with the fewest labels.

What’s the difference between general Spatial-Temporal information and our Spatial-Temporal AU correlation knowledge? Two attention matrices, in Figure 7, contains the relevance of each atomic AU class and frame-level class. By modeling the spatial and temporal AU dependency in attention matrices, the video-level and frame-level AU co-occurrence and mutual exclusive relation is refined and learned to improve the the general Spatial-Temporal information.

Why do we choose transformer? First, self-attention based methods (i.e., JAAnet [35]) have been proved to be very effective in learning AUs semantic relation. Second, the residual connection, multi-head attention, and positional embedding designs make it an efficient tool to learn long-range temporal cues and more discriminative representations. Third, our experiments show that transformer performs better than other popular models such as regular GCNs.

Why do we need both consistency regularization and pseudo-labeling? The consistency regularization is used for building two level knowledge distillation. It distills the fully modeled spatial AU relationship knowledge from branch A to branch B, and distill the temporal AU correlation knowledge from branch B to branch A. However, without pseudo-labeling, some of the Spatial Students stay idle and the unlabeled data is not fully utilized, making the training process less efficient. By combining consistency regularization and pseudo-labeling, KS can accelerate the speed and effect of knowledge distillation and spread.

Why are Spatial Student models based on MLP instead of transformer? In most cases, KS need feed Spatial Student models with unlabeled data, which means the results derived by Spatial Students is less credible. Thus, a weak design of Spatial Student is necessary. In additional, different design of Spatial Student and Spatial Teacher can be recognized as a noise or a model-wise perturbation for better applying the consistency regularization.

Why do we need the temporal constrain for pseudo-labeling? First, automatic AU detection, as a multi-label task, faces some difficulties in selecting and retaining the pseudo labels when only partial labels are with high confidence score. Compared with multi-class tasks, the one-hot format of multi-labels makes

it hard to decide if the pseudo labels are confident in a holistic way or a local way. Setting the temporal constrain makes it easier to filter the cases which are not consist with the regular pattern of facial action movements. Second, the temporal label smoothness is also a soft constrains from human knowledge for better generalizing out-of-distribution AU data.

How to generate pseudo labels? We pick up the class which has maximum predicted probability for each binary class of unlabeled samples.

Can KS be trained with video clips without any labels? If yes, how? Yes, it can. When feeding KS with the unlabeled video clips, we only update our model with the loss of pseudo-labeling and Temporal Teacher. It worth noting that the unlabeled video clips are not allowed to use before the model training is stable (10 epochs in this project). Otherwise learning unreliable knowledge first will lead the model to the error-prone issue.

Why using 20% labels achieves nearly the same performance as using 100% on BP4D? This is due to the large portion of overlapped annotations, using 20% labels with sparsely sampled annotations makes the performance reach the “saturation” quickly, hence there is no significant performance gain after 20% towards the use of 100% labels. Our finding complies with the “less is better” principle confirmed by the other existing works [16].

How about applying different sequential perturbation for the pseudo label confirmation module? The fact is that using or mixing certain perturbations (e.g., temporal feature shift, random mask, and flip) does not bring obvious performance improvement. We speculate that other perturbations can not model the temporal fluctuations caused by incorrect pseudo labels well. Applying inappropriate or excessive perturbation operation can even degrade the performance.

6.3 Inference Strategy

We adopt the inductive learning manner at testing stage. A random key frame number is assigned to each batch of input video clips. Given a video clip, both branch A and branch B are used to extract the feature O_{output} for prediction.

6.4 Additional Implementation Details

All training images in the same video clips are randomly rotated (-45 to 45 degrees), flipped horizontally (50% possibility), and with color jitters (saturation, contrast, and brightness) simultaneously. The detailed specification of Knowledge-Spreader is shown in the original code (model designing part). The complete code will be released to the research community by the time of the paper being published. We choose 5 as the frame length of each input video clip for the optimal time-and-accuracy trading-off. The analysis of the hyper-parameters can be seen in Section 6.6. We implement our Knowledge-Spreader (KS) with the Pytorch framework and perform training and testing on the NVIDIA GeForce 2080Ti GPU.

6.5 Additional Quantitative Evaluation

The quantitative results with different label ratios are shown in Table 4 for reference. It corresponds to Figure 4 in the original paper. In addition, due to the page limitation, only partial comparison results with supervised methods in terms of individual AU are shown in Table 2 of the original paper. Table 5 shows the complete comparison results.

Table 4: Quantitative comparison with semi-supervised methods using F1 score. Underlines indicate the best results of individual models.

Model	BP4D	DISFA	MME	Model	BP4D	DISFA	MME
Pseudo-label (1%)	54.3	40.4	45.8	FixMatch (1%)	49.9	35.6	41.6
Pseudo-label (2%)	57.8	50.8	47.5	FixMatch (2%)	55.1	46.2	46.5
Pseudo-label (5%)	59.7	51.5	52.1	FixMatch (5%)	59.2	52.7	52.6
Pseudo-label (10%)	60.7	56.8	54.2	FixMatch (10%)	60.5	55	55.4
Pseudo-label (15%)	61.2	57.1	54.9	FixMatch (15%)	62.1	57.7	55.6
Pseudo-label (20%)	62	58.5	55.2	FixMatch (20%)	62	58.4	56.4
Pseudo-label (50%)	<u>63.6</u>	57.9	55.3	FixMatch (50%)	62	57.9	<u>58.3</u>
Pseudo-label (60%)	62.7	56.7	55.3	FixMatch (60%)	62.1	56	56.4
Pseudo-label (70%)	63.3	57.9	55.3	FixMatch (70%)	61.9	57.8	57.2
Pseudo-label (80%)	62.4	58.3	56.6	FixMatch (80%)	62.2	56.9	55.5
Pseudo-label (90%)	62.3	57.5	55.5	FixMatch (90%)	61.9	57.5	55.3
Pseudo-label (100%)	62.7	<u>58.8</u>	<u>56.9</u>	FixMatch (100%)	<u>62.7</u>	<u>58.8</u>	56.9

Model	BP4D	DISFA	MME	Model	BP4D	DISFA	MME
TCL (1%)	55.6	42.3	43.3	Our KS (1%)	59.9	64.9	51.2
TCL (2%)	58.9	51.2	48.2	Our KS (2%)	62.5	52.8	54.8
TCL (5%)	60.5	53.6	53.4	Our KS (5%)	63.9	56.9	57.6
TCL (10%)	61.7	55.8	55.7	Our KS (10%)	64.4	58	58.4
TCL (15%)	62.3	56.7	56.2	Our KS (15%)	64.5	58.8	58.7
TCL (20%)	62.7	57.9	55.6	Our KS (20%)	<u>64.6</u>	59.5	58.9
TCL (50%)	<u>63.2</u>	59.2	57.6	Our KS (50%)	<u>64.3</u>	61.4	59.5
TCL (60%)	62.8	60.1	57.9	Our KS (60%)	64.4	62.6	59.2
TCL (70%)	63.0	59.6	57.9	Our KS (70%)	64.5	61.9	58.8
TCL (80%)	62.9	<u>60.4</u>	<u>58.3</u>	Our KS (80%)	64.4	62	59.3
TCL (90%)	62.7	58.3	57.8	Our KS (90%)	64.4	61.9	59.4
TCL (100%)	63.1	59.7	58.1	Our KS (100%)	64.5	<u>62.8</u>	<u>59.7</u>

6.6 Effect of the Video Clip Length n

To investigate the influence of the input clip length, we perform experiments by the proposed model with 10% sparsely sampled annotations on BP4D and DISFA. Figure 8 shows the F1 score curve with n changes. Overall, the performance improve with the n increases from 2 to a certain threshold. A long video clip, on the other hand, results in high computational and memory costs. For optimal trading-off, 5 to 7 is a proper setting for the video clip length n .

6.7 Parameter Scale Analysis

The trainable parameter size of the proposed model is around 25 million, which makes KS a very light-weighted model. Compared with the baseline algorithm

Table 5: Comparison with state-of-the-art methods using F1 score in terms of individual AUs. The upper part is the F1 score on BP4D; The bottom part is the F1 score on DISFA. Bold numbers indicate the best performance.

Model	Used labels	AU1	AU2	AU4	AU6	AU7	AU10	AU12	AU14	AU15	AU17	AU23	AU24	Avg.
DSIN	100%	51.7	40.4	56.0	76.1	73.5	79.9	85.4	62.7	37.3	62.9	38.8	41.6	58.9
JAA	100%	47.2	44.0	54.9	77.5	74.6	84.0	86.9	61.9	43.6	60.3	42.7	41.9	60.0
LP	100%	43.4	38.0	54.2	77.1	76.7	83.8	87.2	63.3	45.3	60.5	48.1	54.2	61.0
ARL	100%	45.8	39.8	55.1	75.7	77.2	82.3	86.6	58.8	47.6	62.1	47.4	55.4	55.4
SRERL	100%	46.9	45.3	55.6	77.1	78.4	83.5	87.6	63.9	52.2	63.9	47.1	53.3	62.9
UGN	100%	54.2	46.4	56.8	76.2	76.7	82.4	86.1	64.7	51.2	63.1	48.5	53.6	63.3
HMP-PS	100%	53.1	46.1	56.0	76.5	76.9	82.1	86.4	64.8	51.5	63.0	49.9	54.5	63.4
FAUDT	100%	51.7	49.3	61.0	77.8	79.5	82.9	86.3	67.6	51.9	63.0	43.7	56.3	64.2
Our KS	15%	58.7	50.3	62.0	79.5	75.4	84.9	87.1	65.9	45.5	62.9	48.3	53.3	64.5
Our KS	100%	55.1	48.9	56.2	77.3	81.8	83.3	86.4	62.6	51.9	61.3	51.0	58.3	64.5
Model	Used labels	AU1	AU2	AU4	AU6	AU9	AU12	AU25	AU26	Avg.				
DSIN	100%	42.4	39.0	68.4	28.6	46.8	70.8	90.4	42.2	53.6				
JAA	100%	43.7	46.2	56.0	41.4	44.7	69.6	88.3	58.4	56.0				
LP	100%	29.9	24.7	72.7	46.8	49.6	72.9	93.8	65.0	56.9				
ARL	100%	43.9	42.1	63.6	41.8	40.0	76.2	95.2	66.8	58.7				
SRERL	100%	45.7	47.8	59.6	47.1	45.6	73.5	84.3	43.6	55.9				
UGN	100%	43.3	48.1	63.4	49.5	48.2	72.9	90.8	59.0	60.0				
HMP-PS	100%	38.0	45.9	65.2	50.9	50.8	76.0	93.3	67.6	61.0				
FAUDT	100%	46.1	48.6	72.8	56.7	50.0	72.1	90.8	55.4	61.5				
Our KS	15%	41.7	53.5	69.7	41.3	46.2	72.0	92.3	54.0	58.8				
Our KS	100%	53.8	59.9	69.2	54.2	50.8	75.8	92.2	46.8	62.8				

EACnet [20], which contains 138 million parameters, Knowledge-Spreader, as a video-level model, reduces considerable parameter (80%) but achieves excellent performance improvement.

7 Supplementary of New MME

7.1 Participants

233 participants were recruited from our University. There are 132 females and 101 males, with ages ranging from 18 to 70 years old. Ethnic/Racial Ancestries include Asian, Black, Hispanic/Latino, White, and others (e.g., Native American).

7.2 Recording System and Synchronization

Our data collection system consists of a 3D dynamic imaging camera system, a thermal sensor, a physiological signal sensor system, and a studio-quality audio recorder. The system setup and synchronization method are basically consistent with BP4D+ [51].

7.3 Emotion Stimulus

Ten tasks were performed to elicit a wide range of spontaneous emotion expression (from positive, to neutral, and to negative) and inter-personal facial action behavior by a professional interviewer. Table 6 illustrates the detailed description for the designed tasks.

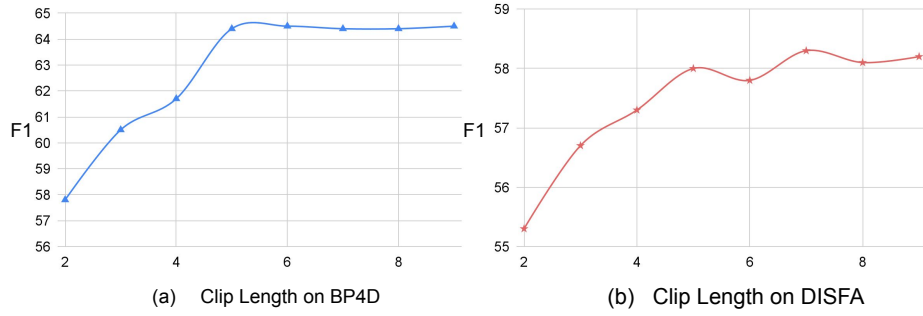


Fig. 8: Effect of the video clip length n . (a) and (b) indicates the F1 score with different video clip lengths on BP4D and DISFA.

Table 6: The stimulus tasks designed for the data collection.

Task ID	Activity	Target Emotion
1	Have a pleasant chat with the interviewer	Happiness
2	Watch a 3D face model of the participant	Surprise
3	Watch an audio recording of 911 emergency call	Sadness
4	Experience a sudden sound from a horn	Startle or Surprise
5	React to a fake news	Skeptical
6	Asked to sing an impromptu song	Embarrassment
7	Experience physical fear of the threat in a dart game	Fear or Nervous
8	Experience the cold feeling by submerging hands into a bucket with ice water	Pain
9	React to the blame from the interviewer	Offended or Unpleasant
10	Experience a bad smell from decaying food	Disgust

7.4 Data Organization

Each subject is associated with 10 different emotions and multi-modal data including the 3D sequence, 2D RGB sequence, thermal sequence, and the sequences of physiological data (i.e., blood pressure, EDA, heart rate, and respiration rate). The sample sequences of different modalities from two subjects are shown in Figure 9. Besides, the metadata including manually labeled action units occurrence and intensity, 3D/2D/IR facial landmarks, and 3D head poses are also generated for better analysis of automatic human facial action.

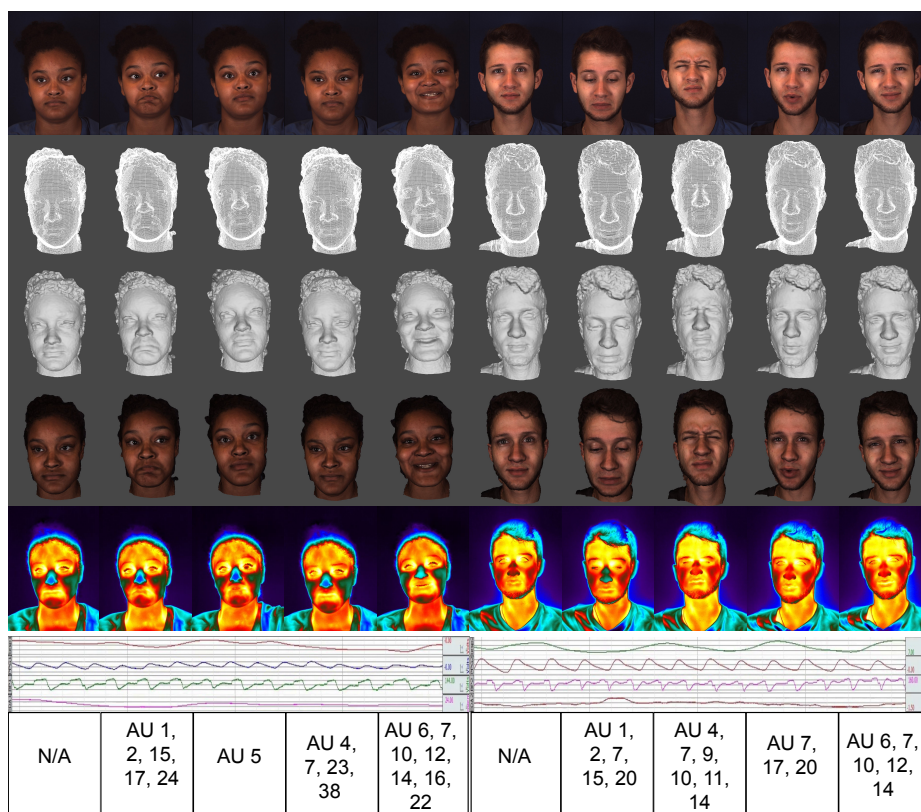


Fig. 9: A sample sequence from our MME. 2D texture image, 3D mesh model, 3D shaded model, 3D texture model, thermal image, and physiological signal (respiration rate, blood pressure, EDA, heart rate) and corresponding AU occurrence are shown from top to bottom.

References

1. Brock, A., De, S., Smith, S.L., Simonyan, K.: High-performance large-scale image recognition without normalization. arXiv preprint:2102.06171 (2021)
2. Choi, J., Sharma, G., Chandraker, M., Huang, J.B.: Unsupervised and semi-supervised domain adaptation for action recognition from drones. In: WACV (2020)
3. Chu, W.S., De la Torre, F., Cohn, J.F.: Learning spatial and temporal cues for multi-label facial action unit detection. In: 2017 12th IEEE International Conference on Automatic Face Gesture Recognition (FG) (2017)
4. Corneanu, C., et al.: Deep structure inference network for facial action unit recognition. In: Proceedings of ECCV (2018)
5. Cui, Z., Song, T., Wang, Y., Ji, Q.: Knowledge augmented deep neural networks for joint facial expression and action unit recognition. In: NIPS (2020)
6. Cui, Z., Zhang, Y., Ji, Q.: Label error correction and generation through label relationships. Proceedings of the AAAI Conference on Artificial Intelligence pp. 3693–3700 (2020)
7. Dosovitskiy, A., et al.: An image is worth 16x16 words: Transformers for image recognition at scale. arXiv preprint:2010.11929 (2020)
8. Guo, Q., Wang, X., Wu, Y., Yu, Z., Liang, D., Hu, X., Luo, P.: Online knowledge distillation via collaborative learning. In: Proceedings of the IEEE/CVF Conference on Computer Vision and Pattern Recognition (CVPR) (2020)
9. He, K., Zhang, X., Ren, S., Sun, J.: Deep residual learning for image recognition. In: Proceedings of the IEEE Conference on Computer Vision and Pattern Recognition (CVPR) (2016)
10. Hinton, G., Vinyals, O., Dean, J.: Distilling the knowledge in a neural network (2015)
11. Huang, Y., et al.: Gpipe: Efficient training of giant neural networks using pipeline parallelism. arXiv preprint:1811.06965 (2019)
12. Jacob, G.M., Stenger, B.: Facial action unit detection with transformers. In: Proceedings of the IEEE/CVF Conference on Computer Vision and Pattern Recognition (CVPR) (2021)
13. Jing, L., Parag, T., Wu, Z., Tian, Y., Wang, H.: Videoss: Semi-supervised learning for video classification. In: WACV (2021)
14. Laine, S., Aila, T.: Temporal ensembling for semi-supervised learning. In: 5th International Conference on Learning Representations, ICLR (2017)
15. Lee, D.H.: Pseudo-label : The simple and efficient semi-supervised learning method for deep neural networks. ICML 2013 Workshop : Challenges in Representation Learning (WREPL) (2013)
16. Lei, J., Li, L., Zhou, L., Gan, Z., Berg, T.L., Bansal, M., Liu, J.: Less is more: Clipbert for video-and-language learning via sparse sampling. In: Proceedings of the IEEE/CVF Conference on Computer Vision and Pattern Recognition (CVPR) (2021)
17. Li, G., Zhu, X., Zeng, Y., Wang, Q., Lin, L.: Semantic relationships guided representation learning for facial action unit recognition. Proceedings of the AAAI Conference on Artificial Intelligence (2019)
18. Li, G., et al.: Semantic relationships guided representation learning for facial action unit recognition. In: AAAI (2019)
19. Li, W., Abtahi, F., Zhu, Z.: Action unit detection with region adaptation, multi-labeling learning and optimal temporal fusing. In: Proceedings of the IEEE Conference on Computer Vision and Pattern Recognition (CVPR) (2017)

20. Li, W., Abtahi, F., Zhu, Z., Yin, L.: Eac-net: Deep nets with enhancing and cropping for facial action unit detection. *IEEE Transactions on Pattern Analysis and Machine Intelligence* (2018)
21. Li, X., Li, Z., Yang, H., Zhao, G., Yin, L.: Your “attention” deserves attention: A self-diversified multi-channel attention for facial action analysis. In: 2021 16th IEEE International Conference on Automatic Face and Gesture Recognition (FG 2021) (2021)
22. Li, Y., Zeng, J., Shan, S., Chen, X.: Self-supervised representation learning from videos for facial action unit detection. In: Proceedings of the IEEE/CVF Conference on Computer Vision and Pattern Recognition (CVPR) (2019)
23. Li, Z., Deng, X., Li, X., Yin, L.: Integrating Semantic and Temporal Relationships in Facial Action Unit Detection (2021)
24. Li, Z., Deng, X., Li, X., Yin, L.: Integrating Semantic and Temporal Relationships in Facial Action Unit Detection (2021)
25. Mavadati, S.M., et al.: Disfa: A spontaneous facial action intensity database. *IEEE Transactions on Affective Computing* 4(2), 151–160 (2013)
26. Mei, C., Jiang, F., Shen, R., Hu, Q.: Region and temporal dependency fusion for multi-label action unit detection. In: 2018 24th International Conference on Pattern Recognition (ICPR) (2018)
27. Niu, X., Han, H., Shan, S., Chen, X.: Multi-label co-regularization for semi-supervised facial action unit recognition. In: NeurIPS (2019)
28. Niu, X., et al.: Local relationship learning with person-specific shape regularization for facial action unit detection. In: Proceedings of the IEEE Conference on Computer Vision and Pattern Recognition (CVPR) (2019)
29. Pantic, M., Valstar, M., Rademaker, R., Maat, L.: Web-based database for facial expression analysis. In: 2005 IEEE International Conference on Multimedia and Expo. pp. 5 pp.– (2005)
30. Park, H., Yoo, J., Jeong, S., Venkatesh, G., Kwak, N.: Learning dynamic network using a reuse gate function in semi-supervised video object segmentation. In: Proceedings of the IEEE/CVF Conference on Computer Vision and Pattern Recognition (CVPR) (2021)
31. Peng, G., Wang, S.: Weakly supervised facial action unit recognition through adversarial training. *Proceedings of the IEEE/CVF Conference on Computer Vision and Pattern Recognition (CVPR)* pp. 2188–2196 (2018)
32. Peng, G., Wang, S.: Dual semi-supervised learning for facial action unit recognition. *Proceedings of the AAAI Conference on Artificial Intelligence* (2019)
33. Russakovsky, O., et al.: Imagenet large scale visual recognition challenge. *International Journal of Computer Vision* (2014)
34. Shao, Z., et al.: Facial action unit detection using attention and relation learning. *IEEE Transactions on Affective Computing* p. 1–1 (2019)
35. Shao, Z., et al.: Deep adaptive attention for joint facial action unit detection and face alignment. In: Proceedings of ECCV (2018)
36. Singh, A., Chakraborty, O., Varshney, A., Panda, R., Feris, R., Saenko, K., Das, A.: Semi-supervised action recognition with temporal contrastive learning. In: Proceedings of the IEEE Conference on Computer Vision and Pattern Recognition (CVPR) (2021)
37. Sohn, K., Berthelot, D., Li, C.L., Zhang, Z., Carlini, N., Cubuk, E.D., Kurakin, A., Zhang, H., Raffel, C.: Fixmatch: Simplifying semi-supervised learning with consistency and confidence. In: NIPS (2020)

38. Song, T., Chen, L., Zheng, W., Ji, Q.: Uncertain graph neural networks for facial action unit detection. *Proceedings of the AAAI Conference on Artificial Intelligence* pp. 5993–6001 (2021)
39. Song, T., Cui, Z., Zheng, W., Ji, Q.: Hybrid message passing with performance-driven structures for facial action unit detection. In: *Proceedings of the IEEE/CVF Conference on Computer Vision and Pattern Recognition (CVPR)* (2021)
40. Song, T., Cui, Z., Zheng, W., Ji, Q.: Hybrid message passing with performance-driven structures for facial action unit detection. In: *Proceedings of the IEEE/CVF Conference on Computer Vision and Pattern Recognition (CVPR)* (2021)
41. Song, Y., McDuff, D., Vasisht, D., Kapoor, A.: Exploiting sparsity and co-occurrence structure for action unit recognition. In: *2015 11th IEEE International Conference and Workshops on Automatic Face and Gesture Recognition (FG)* (2015)
42. Sánchez-Lozano, E., Tzimiropoulos, G., Valstar, M.: Joint action unit localisation and intensity estimation through heatmap regression. In: *BMVC* (2018)
43. Tang, Y., Zeng, W., Zhao, D., Zhang, H.: Piap-df: Pixel-interested and anti person-specific facial action unit detection net with discrete feedback learning. In: *Proceedings of the IEEE/CVF International Conference on Computer Vision (ICCV)* (2021)
44. Wang, X., Zhang, S., Qing, Z., Shao, Y., Gao, C., Sang, N.: Self-supervised learning for semi-supervised temporal action proposal. In: *Proceedings of the IEEE/CVF Conference on Computer Vision and Pattern Recognition (CVPR)* (2021)
45. Wang, X., Zhang, S., Qing, Z., Shao, Y., Gao, C., Sang, N.: Self-supervised learning for semi-supervised temporal action proposal. In: *Proceedings of the IEEE Conference on Computer Vision and Pattern Recognition (CVPR)*. pp. 1905–1914 (June 2021)
46. Wu, S., Wang, S., Pan, B., Ji, Q.: Deep facial action unit recognition from partially labeled data. In: *Proceedings of the IEEE International Conference on Computer Vision (ICCV)* (2017)
47. Xie, S., et al.: Aggregated residual transformations for deep neural networks. In: *Proceedings of the IEEE Conference on CVPR* (2017)
48. Yang, H., Yin, L., Zhou, Y., Gu, J.: Exploiting semantic embedding and visual feature for facial action unit detection. In: *Proceedings of the IEEE/CVF Conference on Computer Vision and Pattern Recognition (CVPR)* (2021)
49. Zhang, X., Yin, L., Cohn, J.F., Canavan, S., Reale, M., Horowitz, A., Liu, P., Girard, J.M.: Bp4d-spontaneous: a high-resolution spontaneous 3d dynamic facial expression database. *Image and Vision Computing* **32**(10), 692–706 (2014)
50. Zhang, Y., Wu, B., Dong, W., Li, Z., Liu, W., Hu, B.G., Ji, Q.: Joint representation and estimator learning for facial action unit intensity estimation. In: *Proceedings of the IEEE/CVF Conference on Computer Vision and Pattern Recognition* (2019)
51. Zhang, Z., Girard, J.M., Wu, Y., Zhang, X., Liu, P., Ciftci, U., Canavan, S., Reale, M., Horowitz, A., Yang, H., Cohn, J.F., Ji, Q., Yin, L.: Multimodal spontaneous emotion corpus for human behavior analysis. In: *Proceedings of the IEEE Conference on Computer Vision and Pattern Recognition (CVPR)* (2016)
52. Zhang, Z., Wang, T., Yin, L.: Region of interest based graph convolution: A heatmap regression approach for action unit detection. In: *ACM MM* (2020)
53. Zhao, K., Chu, W.S., De la Torre, F., Cohn, J.F., Zhang, H.: Joint patch and multi-label learning for facial action unit detection. In: *Proceedings of the IEEE Conference on Computer Vision and Pattern Recognition (CVPR)* (2015)